

Activation of boron nitride nanotubes and their polymer composites for improving mechanical performance

This article has been downloaded from IOPscience. Please scroll down to see the full text article.

2012 Nanotechnology 23 055708

(<http://iopscience.iop.org/0957-4484/23/5/055708>)

View [the table of contents for this issue](#), or go to the [journal homepage](#) for more

Download details:

IP Address: 210.34.4.139

The article was downloaded on 22/02/2012 at 03:16

Please note that [terms and conditions apply](#).

Activation of boron nitride nanotubes and their polymer composites for improving mechanical performance

Sheng-Jun Zhou¹, Chun-Yin Ma¹, Ye-Yong Meng¹, Hai-Feng Su¹,
Zheng Zhu¹, Shun-Liu Deng¹ and Su-Yuan Xie^{1,2}

¹ Department of Chemistry, College of Chemistry and Chemical Engineering, Xiamen University, Xiamen 361005, People's Republic of China

² State Key Laboratory of Physical Chemistry of Solid Surface, Xiamen University, Xiamen 361005, People's Republic of China

E-mail: sldeng@xmu.edu.cn


Received 1 September 2011, in final form 28 October 2011

Published 11 January 2012

Online at stacks.iop.org/Nano/23/055708

Abstract

Boron nitride nanotubes (BNNTs) are inappropriate for further chemical derivatization because of their chemical inertness. We demonstrate covalent activation of chemically inert BNNTs by isophorone diisocyanate (IPDI) to form isocyanate group (NCO)-terminated BNNT precursors with an 'NCO anchor' ready for further functionalization. As identified by Fourier transform infrared spectroscopy, a number of molecules or polymers with –COOH, –OH or –NH₂ groups are readily attached to the activated IPDI–BNNTs. The IPDI–BNNT-involving polymer composites have shown mechanical properties are considerably improved due to the good dispersibility of IPDI–BNNTs in the polymer matrix and the strong interfacial interactions between BNNTs and polymers. The methodology reported here provides a promising method to promote the chemical reactivity of BNNTs and covalently modify polymer nanocomposites with improved mechanical performance.

 Online supplementary data available from stacks.iop.org/Nano/23/055708/mmedia

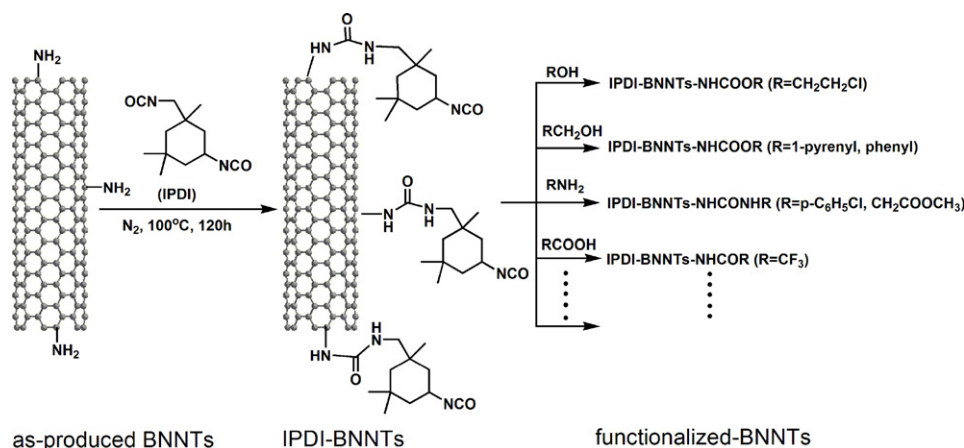
(Some figures may appear in colour only in the online journal)

1. Introduction

Due to the remarkable properties in many aspects, for example, the chirality- and diameter-independent semiconductivity [1–3], the excellent thermal conductivity [3–5], the high elastic modulus [6, 7] and the high resistance to oxidation [3, 8, 9], boron nitride nanotubes (BNNTs) are expected to be attractive candidates for promising applications in composite materials and nanoscale electrical devices working under extreme conditions. However, the limited dispersion of BNNTs in conventional solvents and the poor interfacial interaction with the polymer matrix hinder their applications. In the last few years, many efforts have been devoted to the surface modification towards their dispersibility and surface adhesion improvement [10], including noncovalent processes [11–16] and covalent sidewall functionalization [17–23]. Noncovalent

approaches were achieved through the wrapping of BNNTs using appropriate surfactants or polymers, yet large amounts of surfactant/polymer contaminants may affect their material properties. Moreover, the limited scalability in the noncovalent process is another disadvantage. It heavily depends on covalent functionalization to overcome these problems. However, covalent modification of BNNTs have rarely been investigated chiefly due to their chemical inertness. Promoting the chemical reactivity of BNNTs is thus a key bottleneck and crucial challenge for chemists to functionalize BNNTs.

Here we report a method to activate BNNTs by covalently grafting an isocyanate group (–NCO) onto BNNTs through the reaction of BNNTs with isophorone diisocyanate (IPDI) (scheme 1). The IPDI-activated BNNTs (IPDI–BNNTs) having surviving chemically reactive –NCO groups for further derivatization were characterized essentially by Fourier



Scheme 1. Schematic illustration of the activation and functionalization of BNNTs.

transform infrared spectroscopy (FT-IR). The IPDI-BNNTs can be versatile precursors for reactions with a wide range of functional molecules (e.g. biomolecule, chromophore and medicine) or polymers through the bridge of hydroxyl, amine or carboxylic group. On the basis of activated IPDI-BNNTs, BNNTs/polyvinyl alcohol (PVA) and BNNTs/hydroxypropyl methylcellulose (HPMC) composites were synthesized to render improved mechanical performance as reflected in the forms of Young's modulus and tensile strength.

2. Experiment details

2.1. Materials

Multi-walled carbon nanotubes (MWNTs) were synthesized by chemical vapor deposition [24]. The as-synthesized MWNTs were purified with 2.6 mol l^{-1} HNO_3 under reflux conditions for 24 h. The resulting MWNT materials were copiously washed with deionized water until the effluent was neutral. IPDI was purchased from Bayer Company and kept in a refrigerator at low temperature. Other solvents and compounds used in these studies were commercially available and purified with standard methods.

2.2. Preparation of BNNTs

BNNTs were synthesized by a carbon nanotube substitution reaction [25–28]. Specifically, 260 mg H_3BO_3 and 200 mg MWNTs were milled in a mortar. These powders were then transferred to an alumina combustion boat and loaded into the temperature zone of a quartz tube furnace. The temperature of the furnace was slowly ramped to 1080°C in an argon atmosphere. After that, the argon gas was turned off and anhydrous ammonia with a flow of 120 sccm was simultaneously introduced into the tube furnace. The reaction was allowed to react for 6 h before cooling to room temperature. In order to remove the residual carbon materials, the products were treated at 700°C under the ambient conditions for 5 h to yield the as-produced BNNTs (herein referred to as ap-BNNTs) [26, 28].

2.3. Synthesis of IPDI-activated BNNTs (IPDI-BNNTs)

The synthesis of IPDI-BNNTs was simply based on the chemical reaction between the amine groups on the ap-BNNTs and one of the 'NCO anchors' in IPDI as shown in scheme 1. Specifically, 10 mg ap-BNNTs was added to 2 ml IPDI in nitrogen atmosphere in a round-bottomed flask. The mixture was stirred at 100°C for 120 h. Then the products were sonicated in anhydrous tetrahydrofuran (THF), followed by centrifugation at 8000 rpm for 30 min. In order to completely remove the excessive IPDI, the sediment fractions were repeatedly dispersed in anhydrous THF and then centrifuged at 8000 rpm for four times. The resulting products were dried in a vacuum oven at 50°C for 7 h to yield IPDI-BNNTs.

2.4. Further functionalization of IPDI-BNNTs

The surviving alicyclic isocyanate groups in IPDI-BNNTs make BNNTs chemically reactive for further derivatization and to be versatile precursors for reactions with a wide range of chemicals, including 2-chloroethanol, 1-pyrenyl methanol, benzyl alcohol, *p*-chloroaniline, glycine methyl ester and trifluoroacetic acid. Typically, 10 mg IPDI-BNNTs was reacted with these chemicals in a round-bottomed flask and stirred at $60\text{--}100^\circ\text{C}$ for 120 h under nitrogen protection (table 1). After that, the products were repeatedly dispersed in anhydrous THF and centrifuged at 8000 rpm for four times. The sediment fractions were dried in a vacuum oven at 50°C for 7 h to obtain various functionalized BNNTs.

2.5. Synthesis of BNNT/PVA and BNNT/HPMC composites and fabrication of composite films

A homogeneous PVA solution (with 15 wt% PVA) was obtained by heating a mixture of PVA and dimethyl sulfoxide (DMSO). Specified amounts of IPDI-BNNTs were added to this solution. The mixture was bath-sonicated for 30 min and then kept at 100°C for 120 h. After that, the products were washed with acetone repeatedly and dissolved in hot water to yield an aqueous solution. In order to fabricate

Table 1. Further functionalization of IPDI–BNNTs.

Reactants	Conditions	Products ^a
2-chloroethanol	100 °C/120h	IPDI–BNNT–NHCOOR (R = CH ₂ CH ₂ Cl)
1-pyrenyl methanol in toluene	80 °C/120 h	IPDI–BNNT–NHCOOR (R = 1-pyrenyl)
Benzyl alcohol	80 °C/120 h	IPDI–BNNT–NHCOOR (R = phenyl)
<i>p</i> -chloroaniline in toluene	80 °C/120 h	IPDI–BNNT–NHCONHR (R = <i>p</i> -C ₆ H ₄ Cl)
Glycine methyl ester hydrochloride in THF	60 °C/120 h	IPDI–BNNT–NHCONHR (R = CH ₂ COOCH ₃)
Trifluoroacetic acid	80 °C/120 h	IPDI–BNNT–NHCOR (R = CF ₃)

^a The structural illustrations of the products were presented in supporting information (available at stacks.iop.org/Nano/23/055708/mmedia).

BNNT/PVA composite films, the resulting aqueous solution was dripped onto a glass plate and cooled at room temperature for 24 h, followed by drying in a vacuum oven at 60 °C for 96 h. The composite film was peeled off from the glass plate. In these studies, composite films with 0, 1 and 3 wt% IPDI–BNNTs loading were fabricated. Similarly, composite films with 0, 1 and 3 wt% ap-BNNT loading were fabricated for control experiments. Seven films were fabricated for each sample. The film thickness was controlled in the range of 0.12–0.18 mm.

For BNNT/HPMC composite film preparation, we used *N,N*-dimethylformamide (DMF) as solvent in the replacement of DMSO. Composite films with 0, 1 and 3 wt% IPDI–BNNTs (or ap-BNNTs) loading were fabricated. Seven films with thickness of 0.12–0.18 mm were fabricated for each sample.

2.6. Characterization

The morphologies and structures of the products were characterized by field emission scanning electron microscopy (FE-SEM, LEO1530) and transmission electron microscopy (TEM, TECNAI F-30). Fourier transform infrared spectra (FT-IR) were measured with a Nicolet Avatar 330 FT-IR spectrometer using liquid film (for IPDI, 2-chloroethanol, benzyl alcohol, trifluoroacetic acid) or KBr pellet (for the others) techniques. Thermogravimetric analysis (TGA) were carried out using a TA instrument SDT Q600 thermal analyzer in the temperature ranging from 30 to 600 °C at a heating rate of 10 °C min⁻¹ in air. The mechanical properties of the BNNT–polymer composite films were measured by tensile tests using a Galdabini Sun 2500 machine with a crosshead speed of 5.0 mm min⁻¹. For tensile tests, vacuum oven-dried films were conditioned in the laboratory environment for 24 h before testing. All experiments were performed at room temperature.

3. Results and discussion

3.1. Preparation and characterization of the ap-BNNTs

BNNTs used in these studies were synthesized by the reaction of H₃BO₃ and MWNTs in the presence of anhydrous ammonia at 1080 °C for 6 h [27, 28]. In the reaction,

MWNTs were utilized as templates for the growth of BNNTs, while NH₃ gas not only served as a nitrogen source for the production of BNNTs, but also facilitated the produced BNNT surfaces bonding with amine groups. In addition, the use of ammonia rather than nitrogen in this procedure promised a reaction temperature as low as 1080 °C [27]. The residual carbon materials in the products were got rid of by an oxidation process at 700 °C for 5 h [26, 28]. Figure 1 shows representative SEM and TEM images of BNNTs obtained in the oxidation process. The nanotubes have diameters ranging from 10 to 100 nm and lengths up to tens of microns. As revealed by TEM (figure 1(b)), the ap-BNNTs exhibit well-defined tubular structures with no detectable amorphous coating. The high-resolution TEM (HRTEM) image (figure 1(c)) of the sidewall of a cylindrical BNNT indicates a multi-walled structure with an interlayer distance of ~0.335 nm. XPS spectra (figure 1(d)) recorded from the ap-BNNTs indicate the binding energies of B (1s) and N (1s) at 190.6 and 398.1 eV, which are consistent with the previous investigation about BNNTs [19, 23, 28]. For the B1s peak, a second Gaussian component at 192.1 eV is due to the B–O bonds [29]. The intensities of these peaks give the B:N ratio close to 1:1, confirming the composition of the ap-BNNTs. The additional oxygen and trace carbon observed in the XPS spectra can be ascribed to the residual boron oxide and surface contamination.

3.2. Preparation and characterization of IPDI–BNNTs

In comparison with carbon nanotubes, BNNTs exhibit much lower chemical reactivity because of the very stable B–N bonds [10]. By taking advantage of the amine groups on the surface of nanotubes which might happen to form during BNNT growth in a nitrogenous environment [20, 21] or an ammonia plasma irradiation [18, 19], surface covalent functionalizations were achieved. The IPDI-functionalized BNNTs were simply produced through the chemical reactions between the amine groups on the ap-BNNT surface and the ‘NCO anchors’ in IPDI (scheme 1). Due to the well-crystallized surface, pristine BNNTs are generally difficult to be dispersed in common solvents. However, after IPDI functionalization, BNNTs were shown to be well dispersed in chloroform (figure 2), indicating the successful attachment of IPDI onto the sidewall of BNNTs. The efficient dispersion

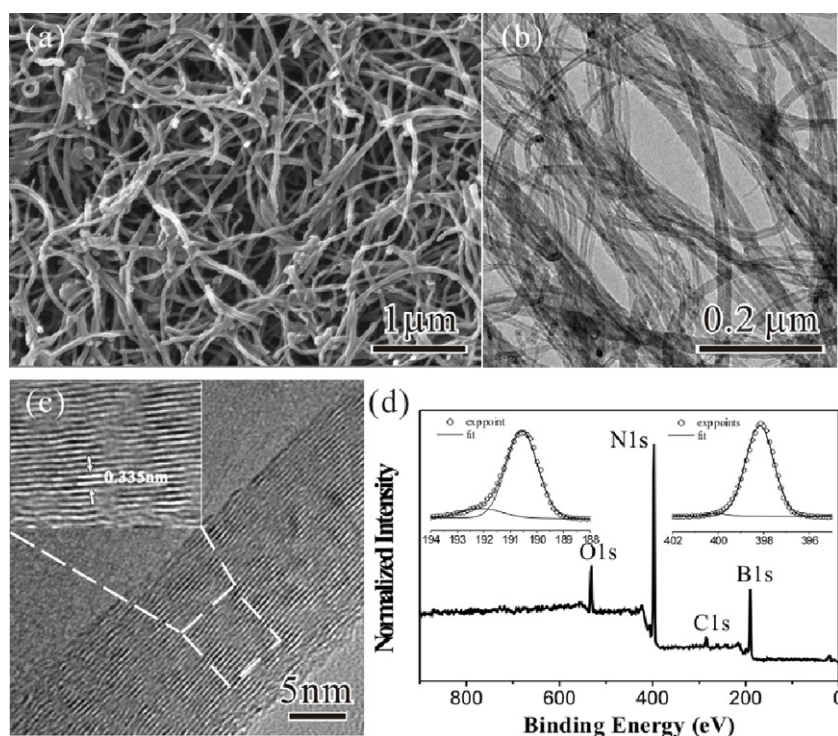


Figure 1. (a) SEM and (b) TEM images of the BNNTs obtained in an oxidation process. (c) HRTEM image of the sidewall of a cylindrical BNNT. (d) Characteristic XPS spectra of the ap-BNNTs.

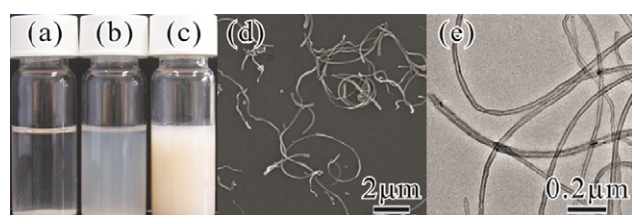


Figure 2. Photographs of the ap-BNNTs (a), IPDI-BNNTs at dilute (b) and concentrated (c) solutions in chloroform after aging for 5 h. SEM (d) and TEM (e) images of the well-dispersed IPDI-BNNTs.

of IPDI-BNNTs was further confirmed by SEM and TEM images (figures 2(d) and (e)), where monodispersed nanotubes were predominant.

As estimated by the weight loss in a temperature range of 220–380 °C in TGA experiment, about 3 wt% of IPDI was loaded on IPDI-BNNTs (figure S1 available at stacks.iop.org/Nano/23/055708/mmedia). Indispensable evidence to identify the IPDI-functionalized BNNTs comes from FT-IR characterization. Figures 3(a)–(c) show IR spectra of reactants (IPDI and ap-BNNTs) and the produced IPDI-BNNTs. The featured absorption at 2265 cm^{-1} in the IR spectrum of IPDI is assigned to the stretching mode of the isocyanate group ($-\text{N}=\text{C}=\text{O}$), while the peaks at around 2920 cm^{-1} are attributed to the alkyl C–H stretching [30]. The spectrum of the ap-BNNTs exhibits two characteristic vibration modes at 1390 and 812 cm^{-1} corresponding to B–N vibrations parallel and perpendicular to the nanotube axis [31]. After IPDI functionalization, three additional IR features around

1632, 2265 and 2958–2926 cm^{-1} appear (figure 3(c)). The appearance of the peak at 1632 cm^{-1} is attributed to the C=O vibration of the urea moiety ($-\text{NH}-\text{CO}-\text{NH}-$) formed from the reaction between the $-\text{NCO}$ group of IPDI and the $-\text{NH}_2$ group in BNNT as depicted in scheme 1. The other two features at 2265 and 2958–2926 cm^{-1} are assigned respectively to the stretching vibration of the isocyanate group ($-\text{N}=\text{C}=\text{O}$) and alkyl C–H in IPDI moieties grafted onto BNNTs [30]. Overall, the IR data provides further evidence for the covalent bonding of IPDI on the surface of BNNTs. More importantly, the IR spectrum of IPDI-BNNTs strongly suggests that a fraction of $-\text{NCO}$ groups remains intact (at 2265 cm^{-1}) in this chemistry.

During the formation of IPDI-BNNTs, the $-\text{NCO}$ groups in IPDI were partially consumed because of their transformation to $-\text{NH}-\text{CO}-\text{NH}-$, while the alkyl C–H in IPDI kept intact. Therefore, measuring the peak area ratio of $-\text{NCO}$ versus C–H groups ($A_{\text{NCO}}/A_{\text{C-H}}$) in both the starting IPDI and the IPDI moiety grafted onto BNNTs allows us to roughly estimate the degree of $-\text{NCO}$ involving in the formation of IPDI-BNNTs. For the starting IPDI, the $A_{\text{NCO}}/A_{\text{C-H}}$ is 1.576, yet the value is decreased to 0.6865 (~44% of 1.576) after grafting on BNNTs, which suggests that ~44% of $-\text{NCO}$ groups still survive in IPDI-BNNTs. Therefore, approximately half of $-\text{NCO}$ groups in IPDI were involved in the reaction with BNNTs for the formation of IPDI-BNNTs.

There are two kinds of $-\text{NCO}$ groups in IPDI, i.e. the aliphatic isocyanate group ($-\text{CH}_2-\text{NCO}$) and the alicyclic isocyanate group ($-\text{NCO}$), directly connected to a

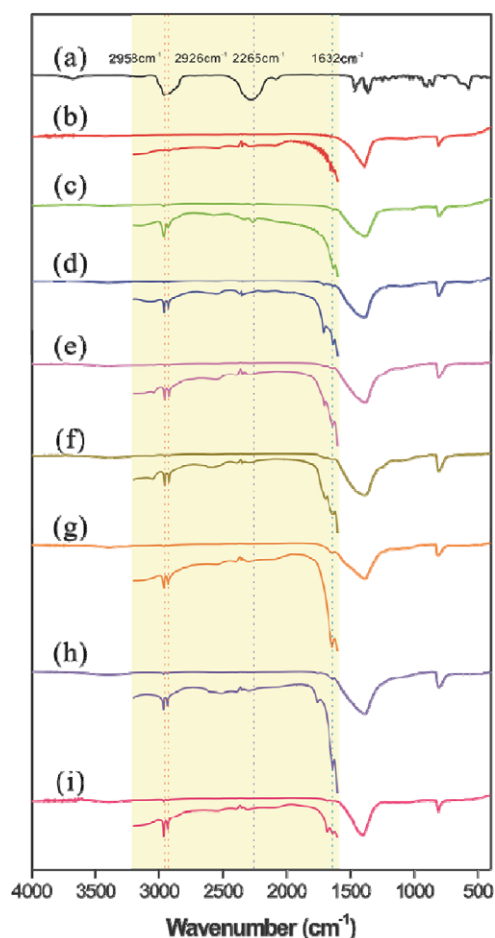


Figure 3. FT-IR spectra of IPDI (a), ap-BNNTs (b), IPDI-BNNTs (c), and functionalized BNNTs with 2-chloroethanol (d), 1-pyrenyl methanol (e), benzyl alcohol (f), *p*-chloroaniline (g), glycine methyl ester (h) and trifluoroacetic acid (i). The insets are the amplified plots (ten times).

six-membered ring. It has been well known that the former is more reactive and sterically favorable than the latter [32]. Accordingly, if only half of -NCO groups in IPDI are involved in the reaction, it is reasonable to assume that the aliphatic isocyanate group preferentially reacts with amine groups on BNNTs and the alicyclic isocyanate group at another side of IPDI remains intact (but we cannot exclude a small fraction of alicyclic isocyanate groups involved in the reaction). It has been shown that the isocyanate group is highly reactive towards various functional groups such as hydroxyl, amine and carboxyl groups. The alicyclic isocyanate groups surviving on the surface of BNNTs are thus ideal 'NCO anchors' open for further derivatization, so as to make BNNTs reactive towards these functional groups in the forms of NCO-terminated IPDI-BNNTs.

3.3. Preparation and characterization of BNNT derivatives based on activated IPDI-BNNTs

BNNTs themselves are chemically inert, but, under otherwise the same reaction conditions, the activated NCO-terminated

IPDI-BNNTs are versatile precursors for further functionalization with various chemicals as well as functional molecules with biological, chromophoric or medicinal performance, including 2-chloroethanol, 1-pyrenyl methanol, benzyl alcohol, *p*-chloroaniline, glycine methyl ester and trifluoroacetic acid (table 1). The reactions between -NCO of IPDI-BNNTs and hydroxyl (amine or carboxyl) groups of these molecules have been unambiguously identified by IR spectra, especially by the C=O vibration in the wavenumber range of $1600\text{--}1800\text{ cm}^{-1}$ (*vide infra*) [30].

Shown in figures 3(d)–(f) are IR spectra of IPDI-BNNT -NHCOOR ($\text{R} = \text{CH}_2\text{CH}_2\text{Cl}$, 1-pyrenyl and phenyl) produced from the reactions of IPDI-BNNTs with 2-chloroethanol, 1-pyrenyl methanol and benzyl alcohol. As compared with the IR spectra of reactants (figure 3(c) for IPDI-BNNTs and figures S2(b)–(d) available at stacks.iop.org/Nano/23/055708/mmedia for hydroxyl compounds), additional signals around 1700 cm^{-1} are observed in these three spectra (figures 3(d)–(f)). The 1700 cm^{-1} is within the featured vibration frequency range of C=O in urethane (-NH-COO-), indicating the functionalized BNNT products bridged with urethane. Similarly, in addition to the original reactant IR peaks (figure 3(c) and figure S2(g) available at stacks.iop.org/Nano/23/055708/mmedia), the appearance of a new band at 1683 cm^{-1} (figure 3(i)) in IPDI-BNNT-NHCOR ($\text{R} = \text{CF}_3$) indicates that the carboxyl group of trifluoroacetic acid reacts with IPDI-BNNTs to form an amide bridge (-NH-CO-). In the case of IR spectra of IPDI-BNNT-NHCONHR ($\text{R} = p\text{-C}_6\text{H}_5\text{Cl}$) produced from the reaction of IPDI-BNNTs and *p*-chloroaniline, however, no additional IR peak is observed in the range of $1600\text{--}1800\text{ cm}^{-1}$ (figure 3(g)). The produced urea bridge vibration is actually overlapped onto the original 1632 cm^{-1} peak of IPDI-BNNTs, leading to an enhanced IR absorption in this area as expected. Similar evidence is observed in figure 3(h), though it should be noted that the weak peaks at 1753 cm^{-1} are due to the original C=O vibration from reactant glycine methyl ester. This evidence also solidifies the conclusion about the urea moiety (-NH-CO-NH-) produced in the formation of IPDI-BNNTs and indirectly validates the existence of -NH_2 in the ap-BNNTs (likely due to the low content, no NH_2 signal is directly observed in the IR spectrum of ap-BNNTs). Actually, no IPDI-boron-nitride derivative was detected if starting from pure boron nitride powders without amine groups.

Another prominent feature of the functionalized BNNT IR spectra (figures 3(d)–(i)) is the disappearance of the 2265 cm^{-1} vibration which has been assigned to the -NCO groups surviving during the formation of IPDI-BNNTs (*vide supra*). This evidence strongly supports the process shown in scheme 1, in which the terminated -NCO groups in IPDI-BNNTs were completely consumed in the following functionalization process.

To investigate the thermal behavior of the functionalized BNNT products, TGA experiments were performed under air conditions. Figure S1 (curve 7 available at stacks.iop.org/Nano/23/055708/mmedia) shows the decomposition curve of 1-pyrenyl methanol-functionalized BNNTs,

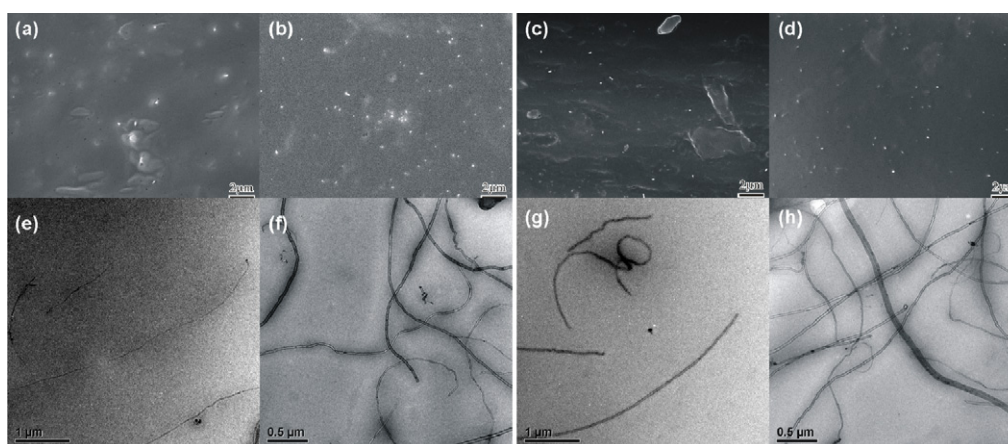


Figure 4. SEM images of the cross sections of BNNT/PVA (a), (b) and BNNT/HPMC (c), (d) composite films, TEM images of BNNT/PVA (e), (f) and BNNT/HPMC (g), (h) composite films ((a), (c), (e), (g), composite films containing 1 wt% IPDI-BNNTs; (b), (d), (f), (h), composite films containing 3 wt% IPDI-BNNTs).

IPDI-BNNT-NHCOOR ($R = 1$ -pyrenyl), in which two distinct decompositions were observed. The first decomposition (below 220°C) with approx. 5.1% weight loss is assigned to the defunctionalization of 1-pyrenyl methanol molecules, while the second one in the temperature range of 220 – 380°C with approx. 4.6% weight loss is assigned to the degrafting of IPDI moieties on BNNTs. The balanceable weight loss in these two decomposition stages agrees well with the proposal about the activated IPDI-BNNTs having half of ‘NCO anchors’ surviving for the next reaction.

3.4. Characterization and mechanical performance of BNNT/PVA and BNNT/HPMC composite films

Based on their excellent properties such as high elastic modulus and thermal conductivity, BNNTs are ideal nanofillers for polymer composite materials with enhanced performance [33–38]. However, the practical applications of BNNT-polymer composites have been limited due to several unsolved problems, for example, the limited dispersibility of BNNTs in the host matrix, the poor interfacial interaction and load transfer between BNNTs and the polymer matrix.

In this work, activated IPDI-BNNTs were used to synthesize BNNT-polymer composites. Figure S3 (available at stacks.iop.org/Nano/23/055708/mmedia) shows the photographs of BNNT/PVA and BNNT/HPMC composite films with different IPDI-BNNT loading. Unlike composite films made from the ap-BNNTs, no nanotube aggregation is observed in the composites synthesized. Together with the TEM images, the SEM images of the cross sections of BNNT/PVA and BNNT/HPMC composite films with different nanotube loadings are shown in figure 4, indicating the BNNTs dispersed well in the polymer matrix.

Tensile tests were performed to evaluate the mechanical properties of these composite films. The typical stress-strain curves, tensile strength and Young’s modulus for pure polymers (PVA and HPMC) and composite films with 1 and 3 wt% BNNT loading, including activated IPDI-BNNTs and ap-BNNTs, are shown in figure 5. It is clear that the

addition of a small fraction of activated IPDI-BNNTs leads to a considerable increase in both Young’s modulus and tensile strength. Specifically, on the addition of only 1 wt% of IPDI-BNNTs, the tensile strength of PVA was increased by 3.6% and the Young’s modulus was increased by 42%. When the loading of IPDI-BNNTs was altered to 3 wt%, the tensile strength was increased up to 22% from 150 to 183 MPa and the Young’s modulus was increased by 49% from 2.19 to 3.27 GPa. However, when ap-BNNTs rather than activated IPDI-BNNTs were used in the fabrication of polymer composite films, different results were obtained in the tensile tests: although the Young’s modulus was increased by the addition of 1 wt% ap-BNNTs, the tensile strength was slightly decreased. When the amount of ap-BNNTs was added up to 3 wt%, both tensile strength and Young’s modulus were decreased. Similar results were yielded in the tensile tests of BNNT/HPMC composite films, in which the addition of a small fraction of IPDI-BNNTs in HPMC, as exemplified by 3 wt%, resulted in the increases of tensile strength (from 73.9 to 94.5 MPa) and Young’s modulus (from 1.63 to 1.92 GPa), yet the addition of 3 wt% of ap-BNNTs in HPMC resulted in the decreases of tensile strength (from 73.9 to 53.4 MPa) and Young’s modulus (from 1.63 to 1.34 GPa).

As described above, activated IPDI-BNNTs exhibit good dispersibility and chemical activity towards various chemicals and functional molecules. Adding IPDI-BNNTs into the solution of PVA or HPMC, the strong interfacial interactions between BNNTs and polymers were achieved by the covalent reactions of hydroxyl groups of polymers and the chemically reactive –NCO groups surviving on the nanotube surface. The covalent binding leads to the homogeneous dispersion of BNNTs in the polymer matrix and results in the reinforcement of the mechanical performance of polymer composites as reflected in the Young’s modulus and tensile strength. In contrast, due to the well-crystallized surface, pristine BNNTs exhibit limited dispersibility and poor interfacial interactions with PVA and HPMC.

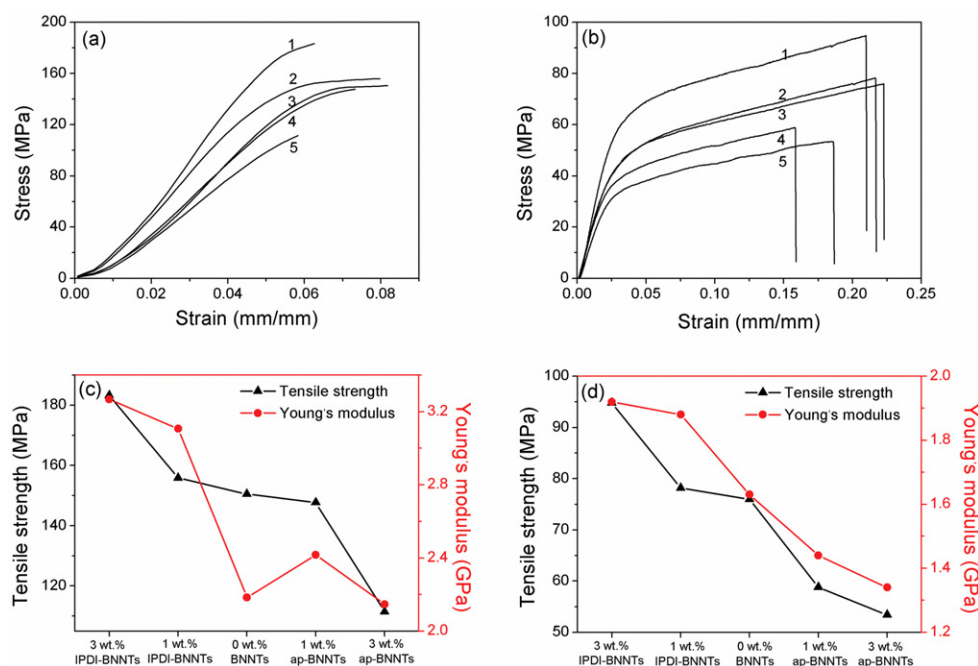


Figure 5. Stress–strain curves of BNNT/PVA (a) and BNNT/HPMC (b) composite films with different BNNT loading (1, 3 wt% IPDI–BNNTs; 2, 1 wt% IPDI–BNNTs; 3, pure PVA or HPMC; 4, 1 wt% ap–BNNTs; 5, 3 wt% ap–BNNTs), tensile strength and Young’s modulus of BNNT/PVA (c) and BNNT/HPMC (d) composite films with different BNNT loading.

4. Conclusions

By taking advantage of the reaction with IPDI, chemically inert BNNTs were activated by covalently grafting isocyanate groups (–NCO) onto their sidewalls. In addition to the dispersibility improvement, the IPDI–BNNTs are versatile precursors with half of the ‘NCO anchors’ ready for further functionalization. A number of molecules with –COOH, –OH or –NH₂ functional groups can be readily attached onto the activated IPDI–BNNTs through the reactions with –NCO groups surviving on the nanotube sidewalls. BNNTs/PVA and BNNTs/HPMC composites based on activated IPDI–BNNTs were synthesized. The tensile tests revealed that the tensile strength and Young’s modulus of the composite films with a small fraction of IPDI–BNNTs were considerably increased. These reinforced mechanical properties were attributed to the good dispersibility of IPDI–BNNTs in the polymer matrix and the strong interfacial interaction between BNNTs and polymers through the covalent reactions of hydroxyl groups of the polymer and the chemically reactive –NCO groups remained on the nanotube surface. Therefore, the current work provides a promising method for promoting the chemical reactivity of BNNTs and producing functional BNNT materials.

Acknowledgments

This work was supported by the 973 Program (no. 2011-CB935901), NSFC (nos. 21021061, 21031004 and 21171140) and the Fundamental Research Funds for the Central Universities (no. 2011121013).

References

- [1] Blase X, Rubio A, Louie S G and Cohen M L 1994 Stability and band gap constancy of boron nitride nanotubes *Europhys. Lett.* **28** 335–40
- [2] Rubio A, Corkill J L and Cohen M L 1994 Theory of graphitic boron nitride nanotubes *Phys. Rev. B* **49** 5081–4
- [3] Golberg D, Bando Y, Tang C and Zhi C 2007 Boron nitride nanotubes *Adv. Mater.* **19** 2413–32
- [4] Xiao Y, Yan X H, Cao J X, Ding J W, Mao Y L and Xiang J 2004 Specific heat and quantized thermal conductance of single-walled boron nitride nanotubes *Phys. Rev. B* **69** 205415
- [5] Kim P, Shi L, Majumdar A and McEuen P L 2001 Thermal transport measurements of individual multiwalled nanotubes *Phys. Rev. Lett.* **87** 215502
- [6] Chopra N G and Zettl A 1998 Measurement of the elastic modulus of a multi-wall boron nitride nanotube *Solid State Commun.* **105** 297–300
- [7] Suryavanshi A P, Yu M-F, Wen J, Tang C and Bando Y 2004 Elastic modulus and resonance behavior of boron nitride nanotubes *Appl. Phys. Lett.* **84** 2527–9
- [8] Golberg D, Bando Y, Kurashima K and Sato T 2001 Synthesis and characterization of ropes made of BN multiwalled nanotubes *Scr. Mater.* **44** 1561–5
- [9] Chen Y, Zou J, Campbell S J and Le Caer G 2004 Boron nitride nanotubes: pronounced resistance to oxidation *Appl. Phys. Lett.* **84** 2430–2
- [10] Zhi C Y, Bando Y, Tang C C, Huang Q and Golberg D 2008 Boron nitride nanotubes: functionalization and composites *J. Mater. Chem.* **18** 3900–8
- [11] Wang W, Bando Y, Zhi C, Fu W, Wang E and Golberg D 2008 Aqueous noncovalent functionalization and controlled near-surface carbon doping of multiwalled boron nitride nanotubes *J. Am. Chem. Soc.* **130** 8144–5
- [12] Velayudham S, Lee C H, Xie M, Blair D, Bauman N, Yap Y K, Green S A and Liu H 2010 Noncovalent functionalization of boron nitride nanotubes with

- poly(*p*-phenylene-ethynylene)s and polythiophene *ACS Appl. Mater. Interfaces* **2** 104–10
- [13] Gao Z, Zhi C, Bando Y, Golberg D and Serizawa T 2010 Isolation of individual boron nitride nanotubes via peptide wrapping *J. Am. Chem. Soc.* **132** 4976–7
- [14] Zhi C, Bando Y, Tang C, Xie R, Sekiguchi T and Golberg D 2005 Perfectly dissolved boron nitride nanotubes due to polymer wrapping *J. Am. Chem. Soc.* **127** 15996–7
- [15] Yu J, Chen Y and Cheng B M 2009 Dispersion of boron nitride nanotubes in aqueous solution with the help of ionic surfactants *Solid State Commun.* **149** 763–6
- [16] Pal S, Vivekchand S R C, Govindaraj A and Rao C N R 2007 Functionalization and solubilization of BN nanotubes by interaction with Lewis bases *J. Mater. Chem.* **17** 450–2
- [17] Xie S-Y, Wang W, Fernando K A S, Wang X, Lin Y and Sun Y-P 2005 Solubilization of boron nitride nanotubes *Chem. Commun.* 3670–2
- [18] Ikuno T, Sainsbury T, Okawa D, Frechet J M J and Zettl A 2007 Amine-functionalized boron nitride nanotubes *Solid State Commun.* **142** 643–6
- [19] Sainsbury T, Ikuno T, Okawa D, Pacile D, Frechet J M J and Zettl A 2007 Self-assembly of gold nanoparticles at the surface of amine- and thiol-functionalized boron nitride nanotubes *J. Phys. Chem. C* **111** 12992–9
- [20] Zhi C, Bando Y, Tang C, Kuwahara H and Golberg D 2007 Grafting boron nitride nanotubes: from polymers to amorphous and graphitic carbon *J. Phys. Chem. C* **111** 1230–3
- [21] Zhi C, Bando Y, Tang C, Honda S, Sato K, Kuwahara H and Golberg D 2005 Covalent functionalization: towards soluble multiwalled boron nitride nanotubes *Angew. Chem. Int. Edn* **44** 7932–5
- [22] Zhi C, Bando Y, Wang W, Tang C, Kuwahara H and Golberg D 2007 Molecule ordering triggered by boron nitride nanotubes and ‘green’ chemical functionalization of boron nitride nanotubes *J. Phys. Chem. C* **111** 18545–9
- [23] Zhi C Y, Bando Y, Terao T, Tang C C, Kuwahara H and Golberg D 2009 Chemically activated boron nitride nanotubes *Chem. Asian J.* **4** 1536–40
- [24] Andrews R, Jacques D, Rao A M, Derbyshire F, Qian D, Fan X, Dickey E C and Chen J 1999 Continuous production of aligned carbon nanotubes: a step closer to commercial realization *Chem. Phys. Lett.* **303** 467–74
- [25] Han W, Bando Y, Kurashima K and Sato T 1998 Synthesis of boron nitride nanotubes from carbon nanotubes by a substitution reaction *Appl. Phys. Lett.* **73** 3085–7
- [26] Han W-Q, Mickelson W, Cumings J and Zettl A 2002 Transformation of B_xC_yN_z nanotubes to pure BN nanotubes *Appl. Phys. Lett.* **81** 1110–2
- [27] Deepak F L, Vinod C P, Mukhopadhyay K, Govindaraj A and Rao C N R 2002 Boron nitride nanotubes and nanowires *Chem. Phys. Lett.* **353** 345–52
- [28] Ma C-Y, Meng Y-Y, Shan G-J, Sun L-C, Lin S-C, Xie S-Y, Huang R-B and Zheng L-S 2011 From graphene sheets to boron nitride nanotubes via a carbon-thermal substitution reaction *Chem. Asian J.* **6** 1331–4
- [29] Kim S Y, Park J, Choi H C, Ahn J P, Hou J Q and Kang H S 2007 X-ray photoelectron spectroscopy and first principles calculation of BCN nanotubes *J. Am. Chem. Soc.* **129** 1705–16
- [30] Mohan J 2004 *Organic Spectroscopy Principles and Applications* 2nd edn (Harrow: Alph Science International Ltd)
- [31] Borowiak-Palen E, Pichler T, Fuentes G G, Bendjemil B, Liu X, Graff A, Behr G, Kalenczuk R J, Knupfer M and Fink J 2003 Infrared response of multiwalled boron nitride nanotubes *Chem. Commun.* 82–3
- [32] Deng J, Zhang X, Wang K, Zou H, Zhang Q and Fu Q 2007 Synthesis and properties of poly(ether urethane) membranes filled with isophorone diisocyanate-grafted carbon nanotubes *J. Membr. Sci.* **288** 261–7
- [33] Zhi C, Bando Y, Tang C, Honda S, Kuwahara H and Golberg D 2006 Boron nitride nanotubes/polystyrene composites *J. Mater. Res.* **21** 2794–800
- [34] Terao T, Bando Y, Mitome M, Zhi C, Tang C and Golberg D 2009 Thermal conductivity improvement of polymer films by catechin-modified boron nitride nanotubes *J. Phys. Chem. C* **113** 13605–9
- [35] Bansal N P, Hurst J B and Choi S R 2006 Boron nitride nanotubes-reinforced glass composites *J. Am. Ceram. Soc.* **89** 388–90
- [36] Zhi C, Bando Y, Terao T, Tang C, Kuwahara H and Golberg D 2009 Towards thermoconductive, electrically insulating polymeric composites with boron nitride nanotubes as fillers *Adv. Funct. Mater.* **19** 1857–62
- [37] Terao T, Zhi C, Bando Y, Mitome M, Tang C and Golberg D 2010 Alignment of boron nitride nanotubes in polymeric composite films for thermal conductivity improvement *J. Phys. Chem. C* **114** 4340–4
- [38] Samanta S K, Gomathi A, Bhattacharya S and Rao C N R 2010 Novel nanocomposites made of boron nitride nanotubes and a physical gel *Langmuir* **26** 12230–6